ELEVENTH SCHOOL ON BIOPHYSICS
OF MEMBRANE TRANSPORT
School Proceedings, Poland, May 4-13, 1992

PATCH-CLAMP MEASUREMENTS OF GAP-JUNCTION CHANNELS IN CULTURED CELLS

Dieter F. Hülser, Reiner Eckert, Günther Zempel, Dietmar Pasche
and Antonina Dunina-Barkovskaya*)
Biology Institute, Biophysics Dept., University of Stuttgart
Pfaffenwaldring 57 D-7000 Stuttgart 80
Federal Republik of Germany
*) A.N. Belozersky Laboratory, Moscow State University, Russia

Introduction

Direct intercellular communication in most tissues is made possible by proteinaceous pores called gap-junction channels. These channels bridge the extracellular gap between apposed cells and connect their intracellular compartments both electrically and metabolically. The extracellular parts of two hemichannels - the connexons - are linked thus forming a communicating gap-junction channel. A detailed characterization of gap junctions is given in the proceedings of the last school [Hülser et al., 1990]. A connexon is a hexamer of protein subunits which are members of the connexin family. Since connexin 32 (Cx32) was the first gap-junction channel protein to be sequenced from hepatocytes, it serves as a reference to which all other gap-junction proteins are compared. In Table 1 many of these connexins are listed; only those proteins which are to a high degree homologous to Cx32 are included. Other channel proteins as a 16 kD protein [Finbow et al., 1988] or a 70 kD protein of lens epithelium [Kistler & Bullivant, 1988] are not considered as members of the connexin family.

The individual channel conductance may vary between 25 and 150 pS. Gap-junction channels of some tissues are more voltage sensitive (e.g. liver) than others (e.g. heart). The question whether these differences in electrical properties may be attributed to the different connexins being expressed in these tissues is still unanswered. Several approaches to resolve this problem will be discussed in this contribution, all are based on double whole-cell patch-clamp measurements using isolated cell pairs, as follows: (1) Cells with two different channel conductances perfused with anti connexin antibodies to specifically block one channel species; (2) Cells with only one connexin species selected by immunological characterization; (3) Weakly coupled HeLa cells transfected with specific connexin genes, a method which resulted in better correlations between connexin type and single channel properties.

Table 1 Members of the connexin family

Connexin	Species	Organ / Tissue	Ref.
26	mouse / rat / human	liver	[11]
30	xenopus	cDNA	[5]
30.3	mouse	skin	[13]
31	mouse / rat	skin	[9]
31.1	mouse / rat	skin	[13],[7]
32	mouse / rat	liver	[10]
33	rat	testes	[7]
37	mouse / rat	lung, kidney	[14]
38	xenopus	embryo	[4]
40	mouse / rat	lung, heart, kidney	[12]
42	rat / dog / chicken	heart	[3]
43	mouse / rat / chicken	heart / fibroblasts	[2]
43	xenopus	embryo	[6]
45	mouse / rat / chicken	heart	[3],[13]
46	rat	lens	[1]
70	rat/rabbit	heart	[8]

[1] Beyer et al., 1988
[2] Beyer et al., 1989
[3] Beyer et al., 1990
[4] Ebihara et al., 1989
[5] Gimlich et al., 1988
[6] Gimlich et al., 1990
[7] Haefliger et al., 1992
[8] Harfst et al., 1990
[9] Hoh et al., 1991
[10] Paul, 1986
[11] Traub et al., 1989
[12] Willecke et al., 1990
[13] Willecke et al., 1991a
[14] Willecke et al., 1991b

Material & Methods

Cell cultures

Nine permanently growing cell lines have been used for our investigations: BRL (ATCC CRL 1442) an epithelioid rat liver cell line; FL (ATCC CCL 62) an epithelioid cell line derived from a human amniotic membrane; BICR/M1R$_k$ [Rajewsky & Grüneisen, 1972] a fibroblastoid mammary tumor cell line of the Marshal rat; 208F [Quade, 1979] a fibroblastoid variant of F2408 Fisher rat cells; MH$_1$C1 (ATCC CCL 144) an epithelioid rat hepatoma cell line; PLC (ATCC CRL 8024) an epithelioid growing human hepatoma cell line; HeLa (ATCC CCL2) a epitheloid cell line derived from a human cervix carcinoma. HeLa cells have also been transfected with specific connexin genes in Dr. Klaus Willecke's laboratory (University of Bonn). We have investigated two transfectants, HeLa K7 transfected with Cx43 and HeLa B35 containing Cx40.

Cell lines were cultivated as monolayers in Dulbecco's modified Eagle's medium or RPMI 1640 (PLC) supplemented with 3.7 g/l $NaHCO_3$, 100 mg/l streptomycin sulfate, 150 mg/l penicillin G, and 10% fetal or newborn calf serum at pH 7.4 and 37°C in a humidified incubator with an 8% CO_2/air mixture.

For the preparation of cell pairs, the culture medium was decanted and the cells were rinsed with phosphate buffered saline to remove serum components. After addition of 1 ml ice-cold trypsin (0.25% in PBS, calcium and magnesium free) to the dish, the cells were incubated between 1 and 10 min at 37°C. Trypsinization was stopped by adding 2.5 ml of culture medium containing 10% serum and the cells were dissociated by gentle agitation with a Pasteur pipette. This suspension was allowed to settle on glass cover slips (14 mm diameter). After 10 min at 37°C, when about 80% of the cells hau attached to the glass, a cover slip was removed from the culture dish, rinsed with Phosphate Buffered Saline (PBS), Krebs Ringer Solution (KRS), Natrium Saline (NS : 130 mM NaCl, 5.4

mM KCl, 1.4 mM $CaCl_2$, 1 mM $MgCl_2$, 10 mM HEPES/NaOH, pH 7.3), or Barium Saline (BS : same as NS but 70 mM $BaCl_2$ instead of NaCl) and transferred into an experimental chamber containing KRS, NS, or BS.

Dye Coupling

The fluorescent dye Lucifer yellow (CH) was injected microiontophoretically into monolayer cells as described in Brümmer et al.(1991). Dye spreading was monitored under a Leitz Standard microscope with phase contrast and epifluorescence equipment.

Current Recording

We have used the double whole-cell patch-clamp technique [Neyton & Trautman, 1985] to study current fluctuations through single gap-junction channels in cell pairs. A schematic circuit (Fig. 1) illustrates the principle of the experimental arrangement.

For double whole-cell measurements the pipette solution consisted of 119 mM KCl, 2.9 mM $MgCl_2$, 5 mM EGTA, and 10 mM HEPES adjusted to pH 7.4 for BRL, FL, PLC and HeLa. The other five cell lines were measured with a pipette solution consisting of 140 mM CsCl, 10 mM TEA, 10 mM EGTA, and 10 mM HEPES (pH 7.33). Current recordings were made using two List EPC-7 patch-clamp amplifiers. Junctional coupling was tested either by square pulses or ramps of voltage. For current to voltage analysis, voltage ramps (0.2 or 0.02 Hz, 50 mV or 100 mV) were applied to one cell while the neighbouring cell was kept at a constant voltage near its resting potential. Current recordings from both cells were lowpass filtered at 250-500 Hz and stored on video tape via a modified digital audio processor [Bezanilla, 1985].

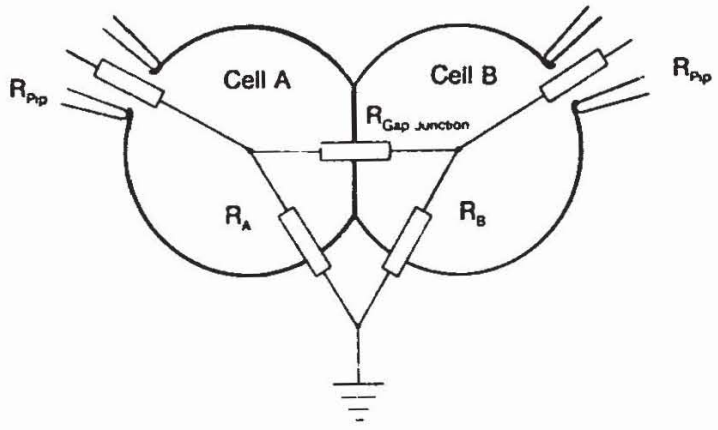

Fig. 1 *Equivalent circuit of double whole-cell recording. R_{pip}: pipette resistance; R_A, R_B: cell membrane resistances; $R_{Gap\ Junction}$: junctional resistance*

Data Processing

Data processing was performed offline using an IBM-AT386 compatible micro-computer equipped with an appropriate A/D-converter board. Programs for acquisition and analysis of patch-clamp data were developed in our laboratory using ASYST. Channel conductances were determined as the slope of the ridges in current-voltage surfaces [Sansom & Mellor, 1990] of these records. We have also estimated the voltage-dependent open probability of the channel within the range of the voltage ramp using a modified I/I_{max} technique. The channel open probability distribution was fitted with a Boltzmann distribution. The equivalent gating charge z and the voltage for half maximal blockage U_0 were estimated and are used together with the channel conductivity to characterize the respective gap-junction channel species. Further details are given in the appendix by R Eckert.

Results

After establishing the double whole-cell patch-clamp recording, cell pairs of FL, BRL, MH_1C_1, PLC, 208F and BICR/M1R_k were found to have cell to cell conductances, $g(t_0)$, between 8 and 80 nS. These initial values decreased within 10 to 50 min so that single channel conductances could be recorded.

We started our experiments with FL and BRL cells where similar current fluctuations through single gap-junction channels have been recorded. These values of 60 and 90 pS may represent individual channels of different connexins. Since BRL is of hepatic origin we probed these cells with antibodies directed against the main hepatic connexins, Cx32 and Cx26. When the antibodies react specifically with the connexins, one of the single channel conductance levels observed should be eliminated so that at the end of an uncoupling experiment only the complementary conductance level should prevail. This, however, was not the case: both antibodies significantly increased the uncoupling effect in BRL cells whereas FL cells only responded to anti-Cx26 antibodies. In no case, however, preference for one of the two conductance levels had been observed [Paschke et al., 1992]. The application of antibody greatly increased the noise level so that single channel events could no longer be observed. A direct correlation between connexin type and channel conductance was, therefore, not possible by antibody injection. We, furthermore, tested the molecular type of connexins present in these two cell lines and western blotting analyses revealed Cx43 as the main gap-junction protein in both FL and BRL cells. This finding would suggest that the antibodies did not block specifically but exerted some cross-reactivity with the Cx43 antigen and/or cytosolic components that interfere with opening or closing of gap-junction channels. Since BRL cells no longer express Cx26 and Cx32 as liver cells do *invivo*, these results also indicate that cells may vary their original connexin type(s) when they permanently grow in culture.

In a second approach therefore we concentrated on cell lines which were characterized by immunoblotting and/or mRNA analyses for their connexin types. The mammary tumor BICR/M1R$_k$ cells which mainly contain Cx43 also have two conductance steps: again 90 pS, which we detected already in BRL and FL cells, and a new one at 120 pS. The rat fibroblast line 208F, which also should contain Cx43 as the main gap-junction protein, revealed four different conductances: a conductance step of 40 pS was present in addition to the three already mentioned values .

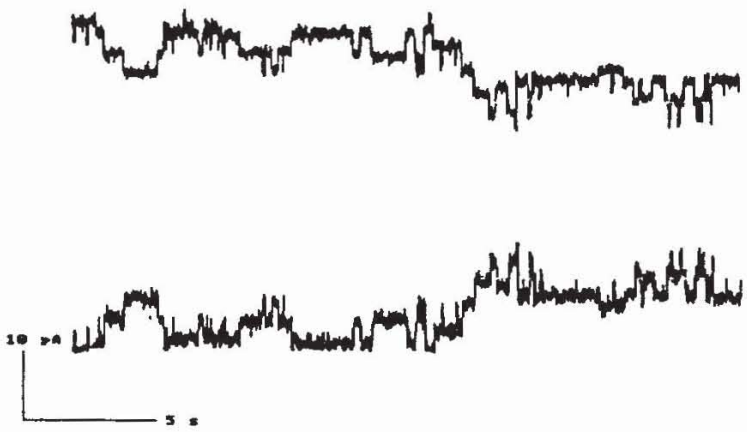

Fig 2a *Current fluctuations through gap-junction channels in a 208F cell pair*

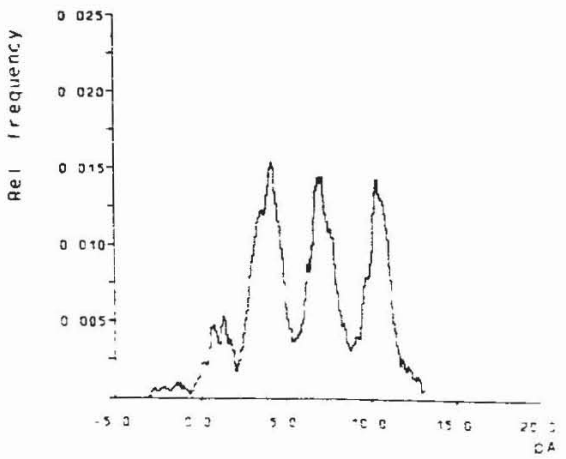

Fig 2b Amplitude histogram of the record in Fig 2a

Current fluctuations at a transcellular voltage of 32 mV in a 208F cell pair are demonstrated in Fig. 2a and the respective amplitude histogram is given in Fig. 2b. The discrete current fluctuations have always been resolved in all cell lines that we investigated when the total junctional conductance had decreased to (or was not more than) 200 pS. These current fluctuations are attributed to the opening and closing of single gap-junction channels and always appear as mirrored deflections in the current records from both cells. In the rat hepatoma line MH_1C_1, which predominantly should contain Cx32, at least three different conductance steps have been resolved (see Table 2). Interestingly, a 25 pS single channel conductance could be identified which is also present in the human hepatoma cell line PLC.

These different conductance steps appeared confusing. Further characterization, however, by additional parameters such as voltage dependence may lead to a better identification of these gap-junction channels. The voltage dependence is demonstrated

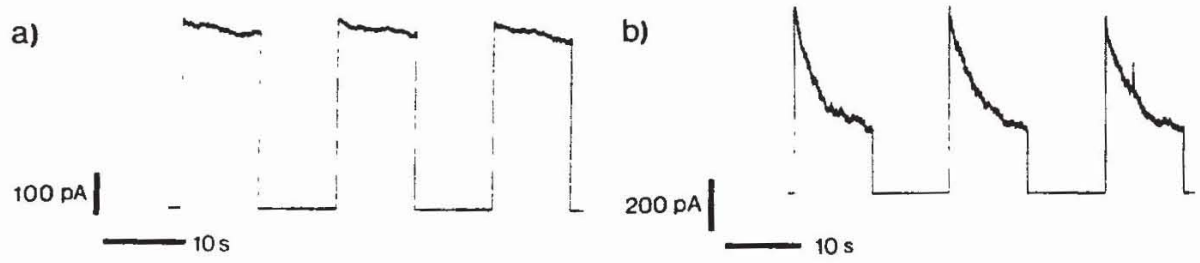

Fig. 3 *Record of total gap-junctional current after rectangular voltage steps in PLC cell pairs. Cells were stepped to transjunctional voltages of 50 mV(a) and 100 mV(b)*

in Fig. 3a and b with PLC cell pairs: after voltage steps to 50 or 100 mV transjunctional voltage, the current necessary to clamp the cell to the selected voltage changed exponentially, indicating a closure and/or reduced open probabilty of gap-junction channels. Measurements at single channel level revealed that the single channel conductance is not changed but the open probability is drastically reduced (see Fig. 4a and b). An amplitude histogram as is shown in Fig. 2b can, therefore, only represent the

channels' activity at a given transjunctional voltage. Instead of voltage pulses, ramps can be used which allow a continuous recording of the voltage dependence of either total junctional conductance (Fig. 5a) or single channel conductance (Fig. 5b).

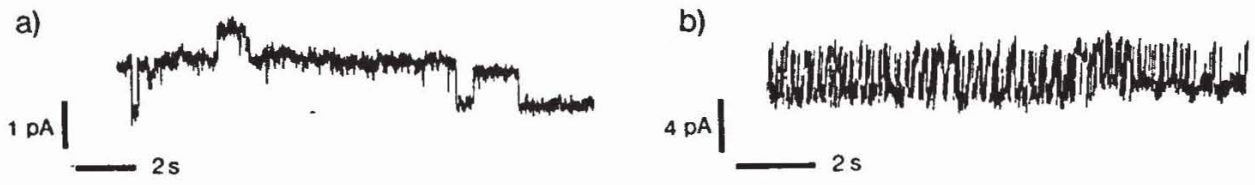

Fig. 4 *Voltage dependent gating of single gap-junction channels in PLC cell pairs. Transjunctional voltage was 40 mV (a) and 65 mV (b)*

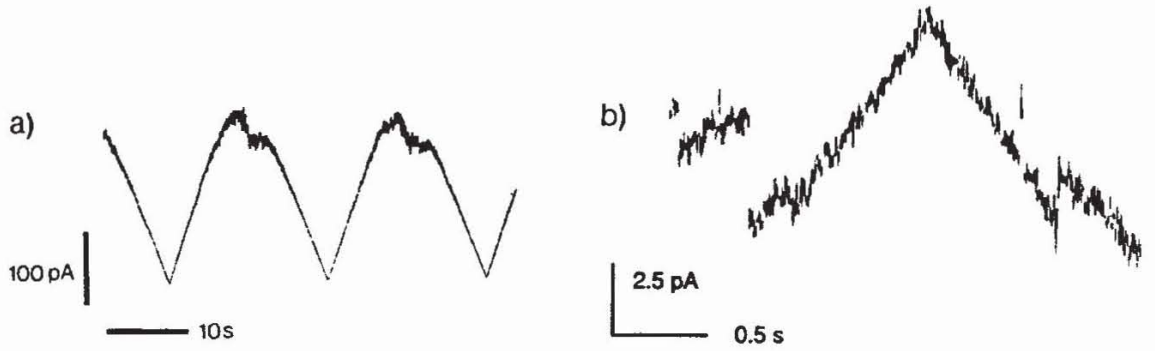

Fig. 5 *Current recordings from PLC cell pairs where transjunctional voltage ramps of 100 mV were applied. a) Total junctional conductance. b) Single channel conductance*

With some modifications for the calculation of channel open probabilities, an appropriate analysis program has been developed which allows the presentation of two dimensional histograms (current-voltage surfaces) as 3-D or 2-D plots (for details see appendix). In Fig. 6 a current-voltage surface is demonstrated in a 3-D representation for single channel data of PLC cells, and in Fig. 7 the corresponding contour plot is shown from where two conductance states (30 pS and 60 pS) can be obtained.

The channel open probability distribution was estimated from these data, revealing a superposition of two different Boltzmann distributions (Fig.8). Voltages for half

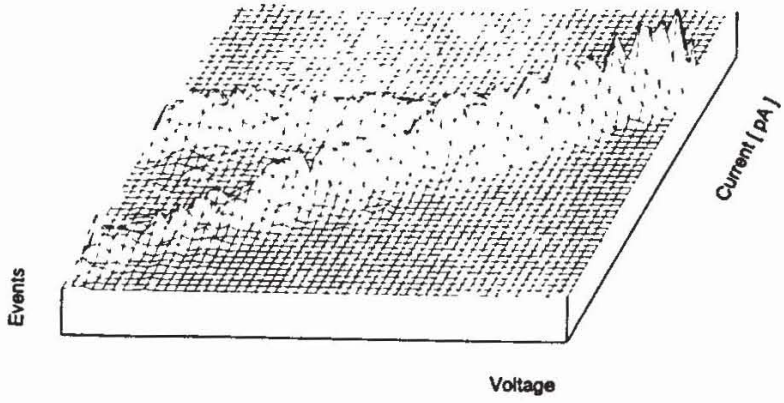

Fig. 6 *3-D representation of a current-voltage surface from the data in Fig. 5b*

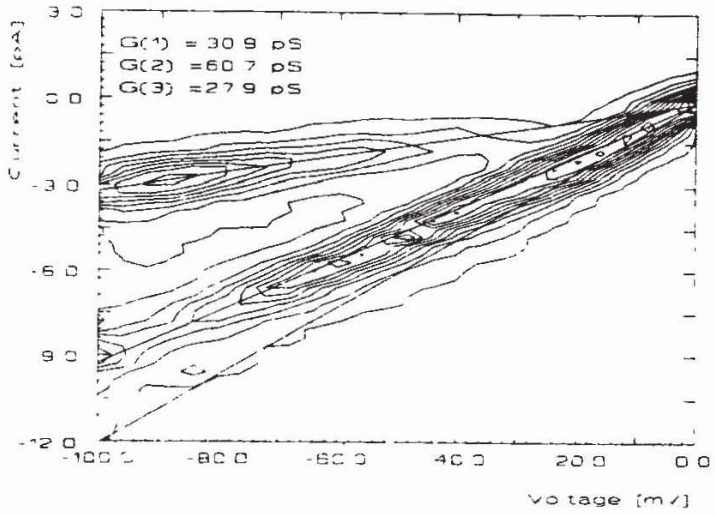

Fig. 7 *Contour plot corresponding to Fig. 6*

maximal blockage (U_0) were -22.7 mV and -48.9 mV, with the respective gating charges z of -2.9 and -1.4. These data could not be correlated with specific gap-junction channel types without additional information. We, therefore, looked for non coupled cells which could be transfected with a single connexin gene. Since Lucifer yellow is retained in some cells, even though they are coupled with a considerable (1-2 nS) transcellular conductance [Paschke, 1989], we reinvestigated with high resolution measurements several cell lines known to be "uncoupled" with respect to dye spreading or ionic coupling as determined with inserted microelectrodes. So far, with the double whole-cell patch-clamp

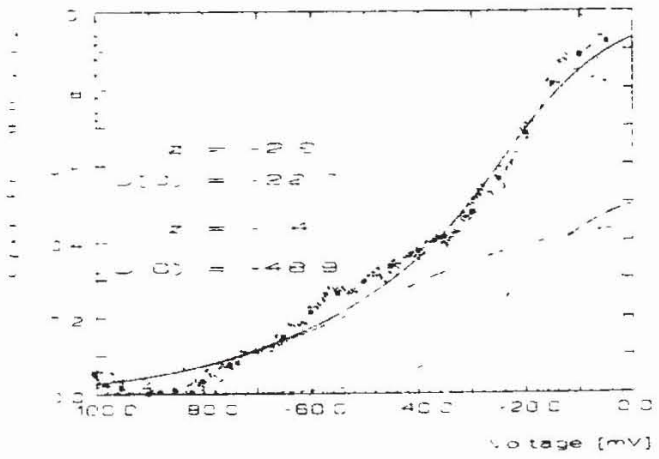

Fig. 8 *Open probability distribution for gap-junction channels in PLC cell pairs*

technique we did not find any permanently growing cell line without gap junctional coupling.

One of these permanently growing cell lines is the human cervix carcinoma HeLa which do not allow Lucifer yellow spreading [Bräuner et al., 1990]. With high resolution current recording, however, very low junctional conductances can be measured in monolayers of HeLa cells. In 34% of the measurements (n = 75) conductances of about 500 pS were observed; only in 4% of the cases, junctional conductance was above 1 nS - the rest had no detectable coupling. Due to the low initial conductance, single channel currents can be observed between neighbouring cells in HeLa monolayers without any pre-treatment. For the record shown (Fig. 9), square pulses of 50 mV were applied. Single channel currents had amplitudes of 1.7 pA corresponding to 34 pS single channel conductance. Total conductance was about 200 pS corresponding to about 8 active channels in this cell junction. From the current-voltage surface (Fig. 10) single channel conductances of 25 ± 4 pS can be estimated for gap-junction channels in HeLa cells.

Gap-junction channels in HeLa cells also show voltage-dependent gating (Fig. 11). However, the voltage-dependent component was about 50% of the total open probability.

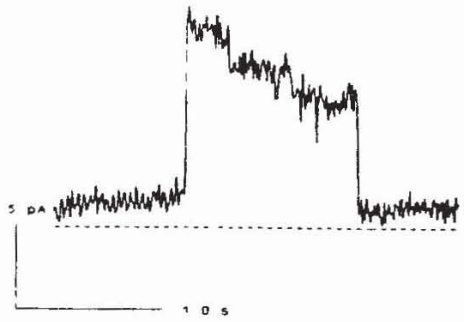

Fig. 9 *Single channel currents of gap-junction channels in HeLa cells grown in a monolayer. Cells were stepped to 50 mV transjunctional voltage*

The maximal open probability at 0 mV was only about 0.6, indicating additional voltage-independent components. Mean gating parameters for the voltage-dependent gate were determined as equivalent gating charge z = 2.5 ± 0.4 and voltage for half maximal blockage U_0 = 42 ± 6 mV [Dunina-Barkovskaya et al., 1992].

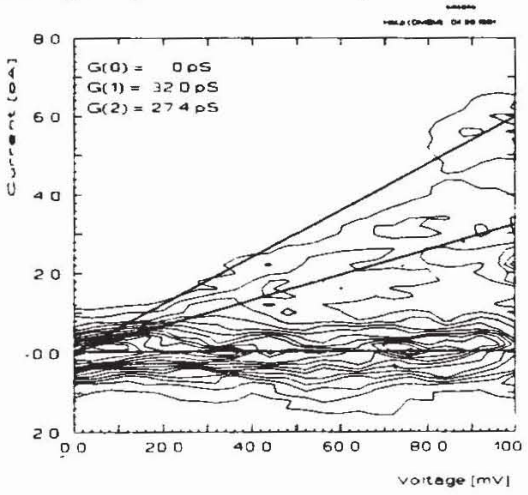

Fig. 10 *Current-voltage surface of single gap-junction channels in HeLa cells*

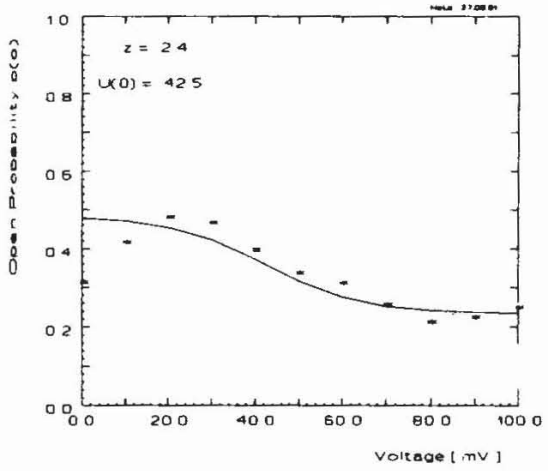

Fig. 11 *Open probability distribution of gap-junction channels in HeLa cells*

This HeLa cell line was transfected with Cx40 and Cx43 and again analyzed for gap junctional coupling under high resolution double whole-cell patch-clamp measurements.

HeLa cells transfected with Cx43 - the main connexin found in BRL, FL, BICR/M1R$_k$ and 208F - revealed in every case a total junctional conductance of >15 nS and a single channel conductance of 60 pS which was also present in the other investigated cell lines. The fitting of the open probability gave a voltage for half maximal blockage of 72.5 mV and an equivalent gating charge of 2.4. Transfection with Cx40 which is predominantly found in lung tissue resulted in total junctional conductances of > 10 nS and in a single channel conductance of 150 pS with U_0 = 50 mV and z = 4.6. In both transfected cell lines Lucifer yellow spreads to a very high degree. All data are summarized in Table 2.

Discussion

Gap junctions provide a path for intercellular communication during embryonic development long before hormonal and neuronal signal transfers are established. Cells in adult organs or tissues are always coupled by gap junctions. The type of connexin(s), however, varies in different tissues or organs, can be differently expressed after hormonal stimulation [Risek et al., 1990; Winterhager et al., 1991], and may change during development and maturation [Dermietzel et al., 1989].

It is impossible to measure the conductance of individual gap-junction channels in intact organs or tissues. The ideal situation for single channel measurements is given in an isolated cell pair, where the electrical paths are simple and - when the cells are small enough - a tolerable background noise from other membrane currents will enable the detection of single gap-junction channel events. This is also true for most cell cultures. Obviously, cells which have been cultured for many years may lose their organ specific type of gap-junction protein(s) and express other connexin(s) which are not found in the parental tissue. This prevents a correlation between connexin type and single channel properties since several possibilities of mixed gap-junction channels may occur, as shown schematically in Fig 12.

Table 2 Gap-Junction Single Channel Conductances in Cultured Mammalian Cells

cell line	main conductance steps / pS				
	30	60	90	120	150
FL human amniotic					
BRL rat liver					
MH_1C_1 rat hepatoma					
PLC human hepatoma	z = 1.8 U_0 = 50mV ?	z = 2.9 U_0 = 25mV ?			
208F rat fibroblast					
BICR/M1R_k rat mammary tumor					
HeLa parental human cervix carcinoma	z = 2.5 U_0 = 42mV				
HeLa K7 transfected with Cx43		z = 2.5 U_0 = 73mV			
HeLa B35 transfected with Cx40					z = 4.8 U_0 = 50mV

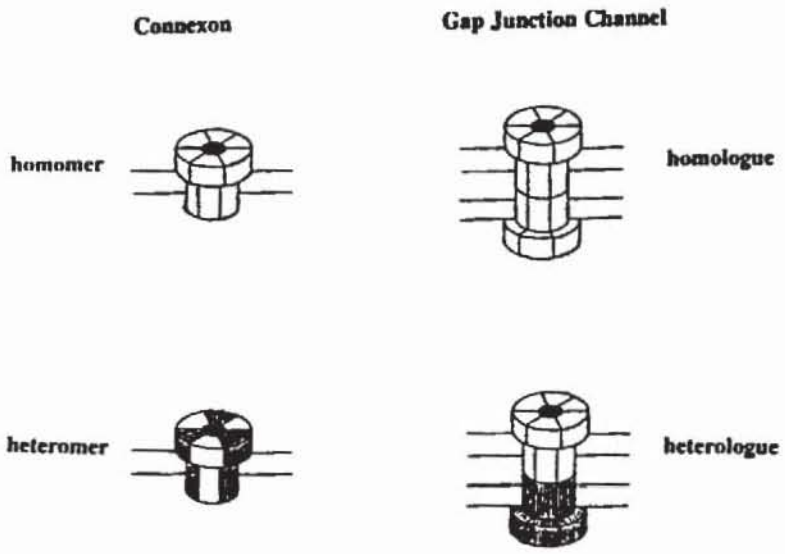

Fig. 12 *Possible subunit arrangements in connexons and gap-junction channels*

Functional blockage of gap-junction channels by injection of antibody directed against a specific connexin must be considered as a useless tool for such a correlation. As we have shown with BRL cells, antibodies directed against Cx26 or Cx32 may block junctional transfer but do not eliminate specifically a single channel conductance level. This block may be a result of cross reactivity of the antibody either with other connexin types and/or cytosolic components involved in the regulation of gap junctional conductance.

A better approach to characterize connexin types by their single channel properties seems to be transfection of non coupled cells with one specific connexin type only. Unfortunately, high resolution measurements of gap junctional conductance always revealed some small amount of endogenous coupling even in "uncoupled" cell lines. One has to select, therefore, a suitable cell line with tolerable "background" coupling, typically less than about 5% of the expected coupling rate after transfection. HeLa cells seem to be such a cell line and our results with transfected cell pairs indicate that connexins can be expressed to a very high degree by transfection. Endogenous channels, therefore, do

not significantly interfere with single channel properties measured in transfected cells. In this situation, there is a high probability of a correlation of single channel conductances with transfected connexins.

Comparison of our measurements of HeLa cells transfected with mouse Cx43, and results with SKHep1 cells transfected with human Cx43 [Moreno et al., 1991] reveal an identical conductivity of 60 pS. In SKHep1 transfectants, however, an additional level of 90-100 pS was described which we were not able to demonstrate in HeLa cells. Whether this is cell specific, or due to the different species origin of the connexin genes, remains to be investigated.

Transfected cell lines also allow the investigation of single channel properties for heterologous and heteromeric coupling and thus enable a better understanding of the heterogenous conductance levels which have been found in many non-transfected, strongly coupled cell lines.

Appendix

CURRENT-VOLTAGE ANALYSIS OF SINGLE CHANNEL CURRENTS USING VOLTAGE RAMPS

R. Eckert

Voltage-dependent gating is a common feature found in many ion channels of excitable cells. For example, in the axonal membrane, voltage gated sodium and potassium channels provide the main mechanism for the propagation of action potentials along the nerve fibre. Voltage-dependent calcium channels in muscle are known to play a significant role in muscle contraction [Hille, 1984]. Biophysical and physiological

aspects of this phenomenon have been studied intensivly and are now well understood at both structural and functional levels [for review see Hille, 1984; Stühmer, 1990]. There is even some evidence that channels which were mainly activated by chemical stimuli (e.g. the nicotinic acetylcholine receptor) show voltage-dependent behaviour [Magleby & Stevens, 1972].

Application of linear voltage ramps is convenient for demonstrating both single channel conductance [Yellen, 1982] and voltage-dependent gating of single channels [e.g.: Schwarze & Kolb, 1984]. No attempt was made, however, to use this method for the quantification of voltage-dependent channel gating. Sansom and Mellor [1990] introduced two-dimensional amplitude histograms, so called "current-voltage surfaces", to study voltage-dependent gating of ion channels assembled from two pore forming peptides in planar lipid bilayers. They suggested fitting the current-voltage surface with appropriate model equations to estimate voltage-dependent gating parameters. Here I report a different approach, which uses an adaption of the standard $\hat{I}/I_{max}$ ratio technique for nonstationary data analysis [Aldrich & Yellen, 1983] leading to a more direct estimate of the voltage-dependent open probability.

Theory

For a brief description of the theoretical background of this method, let us assume the following simple two-state reaction scheme for channel gating:

$$open \underset{k_{co}}{\overset{k_{oc}(U)}{\rightleftharpoons}} closed \qquad (1)$$

For simplicity, only the closing rate k_{oc} should depend on the apparent voltage U in this system . The open probability p_o of the channel is then given as:

$$p_o = \frac{k_{oc}}{k_{oc} + k_{co}} = \frac{[open]}{[open] + [closed]} \tag{2}$$

where the square brackets indicate the total time spent in the respective state(s).

If the system is in thermodynamic equilibrium, i.e. with stationary recordings, it can be shown that:

$$\bar{I} = Nip_o \tag{3}$$

where $\bar{I}$ is the average current over a very long (ideally infinite) duration, N is the number of active channels, i is the unit current of an open channel. Note that in this case the channel open probability p_o is constant.

Since the unit current of the channel is $i = \gamma U$ (where γ is the unit conductance of the channel) eq. (3) may be rewritten as:

$$\bar{I} = N\gamma Up_o \tag{4}$$

This notation implicitly assumes a homogeneous population of ion channels. However, if the channel population is inhomogeneous and consists of j subpopulations, the average current is given as the sum

$$\bar{I} = \sum_{j=1}^{J} N_j \gamma_j U p_{oj} \tag{5}$$

where N_j is the number of channels of the jth subpopulation, γ_j is the channel conductance of this subpopulation of channels and p_{oj} is their open probability.

With stationary records, p_o is assumed to be time invariant. However, eq. (3) also holds for nonstationary data. Thus, if channel gating is voltage-dependent and if the command voltage is changed, e.g. by applying ramps, eq. (4) must be written as

$$\hat{I}(U) = N\gamma Up_o(U) \tag{6}$$

Here, $\hat{I}$ represents the average current from an ensemble of similar data [Aldrich & Yellen, 1983]. If all channels are open (i.e., if $p_o = 1$), the maximum current is given by

$$I_{max} = N\gamma U \tag{7}$$

Therefore, the open probability can be expressed as the ratio of currents

$$p_o(U) = \frac{\hat{I}(U)}{I_{max}} \tag{8}$$

which is equivalent to the ratio I_∞/I_0 used in current relaxation experiments with voltage pulses. With linear voltage ramps, however, I_{max} and $\hat{I}$ can be obtained for the total voltage range of the ramp within a single experiment where I_{max} is determined from the current-voltage surface simply as the component with the highest conductance. The values obtained for p_o can then be plotted versus the applied command voltage.

For voltage gated channels the open probability distribution can be related to the change in (electrical) energy between open and closed state via the Boltzmann equation [Hille, 1984]

$$p_o(U) = \frac{1}{1 + e^{\frac{zq_e}{kT}(U - U_0)}} \tag{9}$$

where q_e is the elementary charge, k is the Boltzmann constant and T the absolute temperature. U_0 is the voltage for half maximal blockage i.e. when U is set to U_0, the exponential term is 1 and $p_o = 1/2$. The parameter z determines the maximal slope in the decline of the open probability distribution and is usually interpreted as an equivalent gating charge that moves across the membrane. This open probability distribution $p_o(U)$ may be fitted with a Boltzmann distribution to estimate z and U_0 of the channels voltage gate. Again, this assumes a homogeneous population of channels (or gates). For an inhomogeneous population of channels eq. (9) has to be modified to

$$p_o(U)_{app} = \sum_{j=1}^{J} f_j \frac{1}{1+e^{\frac{z_j q_e}{kT}(U-U_{0,j})}} \qquad (10)$$

where f_j is the contribution to the total conductance of the subpopulation j of channels.

Data Recording

We have used the double whole cell recording technique [Neyton & Trautman, 1985] to study current fluctuations through single gap-junction channels in isolated cell pairs. Current records were low pass filtered at 250-500 Hz with an 8-pole Bessel filter (Frequency Devices 902 LPF, Haverhill, MA) and stored on video tape, via a modified Sony PCM-501 digital audio processor [Bezanilla, 1985]. Since this system provides only two dc-inputs, it is not possible to record the currents and voltages of two cells concurrently. For voltage ramp experiments, therefore, we used the audio input of a video recorder (Philips VR6762) to store trigger pulses to mark the start and end of each ramp. Since the start and endpoint voltages for each ramp are known, the respective waveform can be reconstructed numerically.

Data Processing

Data processing was performed offline using an IBM-AT386 compatible micro-computer equipped with a Data Translation DT2821F A/D-D/A interface (Stemmer Electronics, Munich, FRG) and a floating point coprocessor to enhance computation speed. Programs for acquisition and analysis of patch-clamp data were developed in our laboratory using ASYST (Keithley Asyst, Rochester, NY), a Forth like programming language with built-in support for most data acquisition and analysis purposes.

For current to voltage analysis the data are sampled in sweeps of 1024 points per trace with the pulse from the audio trace serving as a trigger signal. Each data file

consists of an ensemble of 50 - 100 current records each of which corresponds to one voltage ramp. These ensembles are then processed according to the following scheme to get an estimate of the voltage-dependent open probability of the channel within the range of the voltage ramp.

- Compute the current to voltage surface and the current average at each voltage.
- Determine the base line and maximum current from the current to voltage surface.
- Subtract the base line from each I_{max} and $\hat{I}$ at each respective voltage to get the true values for these quantities.
- Compute the voltage-dependent open probability by dividing $\hat{I}$ by I_{max}.
- Fit the result with eq. (9) or (10) to estimate z and U_0.

Curve fitting is done using the simplex minimization procedure [Nelder & Mead, 1965; Caceci & Cacheris, 1984] with a robust estimator for the goodness-of-fit [Press et al., 1989].

Conclusion

Estimation of channel open probability from single channel data usually involves fitting of binomial distributions to the amplitude histograms of stationary recordings [see Sachs & Auerbach, 1983; Horn, 1991]. To establish a complete open probability distribution, it is necessary to analyze a large number of single channel records at different voltages. Very often this cannot be obtained from the same experiment due to limited stability of the patch or "rundown" of channel kinetics. In addition, with binomial estimation of the channel open probability, the number of active channels must be known quite accurately. This is difficult to achieve, especially for large channel numbers and low open probability. In this case, the binomial distribution approaches the Poisson distribution and the number of channels and the open probability are combined into a

single parameter ($\lambda = Np_o$) and, therefore, cannot be separated by the fitting procedure [Horn, 1991; Sachs & Auerbach, 1983]. With different populations of channels which have different conductivities and gating parameters the data have to be fitted by multinomial distributions which have many more parameters and, therefore, the results become less reliable.

Another approach to characterize voltage-dependent channel gating with voltage clamp analysis of (macroscopic) membrane currents is to apply voltage pulses of different amplitude and determine the ratio I_∞/I_0 of the resulting current relaxations. This technique is fast and conveniently done using computer equipment. Since a very large number of different channels may contribute to the total current, interpretation of the results is less straightforward than single channel data [Aldrich & Yellen, 1983]. It is to some extent possible to apply similar techniques to single channel analysis; however, as channel gating is a stochastic process, the average of a great number of similar records have to be used.

By including the information from voltage ramps in two dimensional amplitude histograms - so called "current-voltage surfaces" - Sansom & Mellor [1990] demonstrated an elegant way to analyse both single channel conductivity and voltage-dependent gating. These surfaces contain the same information for a continuum of voltages as one dimensional amplitude histograms for a single voltage. It should be possible, therefore, to employ them for single channel analysis of voltage gated channels though no detailed procedure has been given for this analysis so far. Sansom and Mellor [1990] suggested direct fitting of two dimensional equations describing voltage-dependent channel gating to current-voltage surfaces. The required model equations, however, still involve determination of the binomial open probability and will have to cover a two dimensional data set. Fitting these data will be computationally demanding and is beyond the scope

of conventional personal computers which are regarded as the main type of computer equipment available in most laboratories.

Here I have used a different approach which combines the current amplitude information of current-voltage surfaces with the $\hat{I}/I_{max}$ ratio technique [Aldrich & Yellen, 1983] and so avoids calculation of two dimensional distributions. The data used to construct current-voltage surfaces are, in essence, ensembles. The ensemble average current $\hat{I}$ can easily be calculated concurrently with the current-voltage surface from where I_{max} can be obtained. The experimental procedure employed for this analysis is fast and can conveniently be established using conventional laboratory equipment. It works very efficiently. For example, good estimates for the channel open probability distribution can be obtained from as few as 50-200 ramps if multiple channels are present (about 5-20 min depending on sweep length). It is even possible to analyze different populations of channels in the same patch, if their gating parameters are sufficiently separated, as the method makes no assumption on the statistical distribution of current amplitudes.

The application of this procedure to computer simulated data confirmed that it works reliably even in situations where conventional methods are difficult to apply. So far, this method fails to work only for channels with inactivation kinetics. Another problem, which is not inherent to this method, arises from curve fitting of the resulting open probability distribution with Boltzmann functions. The parameters of the Boltzmann distribution are nonorthogonal so, even for the simple case of a single Boltzmann function, fitting is difficult and the estimated parameters need not be consistent through several repetitions. From the simplex fitting routine used in this study it appears wise to repeat curve fitting several times with different starting values for the model parameters to confirm convergence to a global minimum. Although it is possible to some extent to judge

convergence from visual inspection of the resulting fit, the fitted parameters were found to deviate by about 5% from those given for the simulation even in the best cases.

This method was established in our laboratory mainly to facilitate the analysis of voltage-dependent gating in gap-junction channels. Due to the special nature of cell-cell channels it is not possible to access them with conventional patch-clamp techniques. Instead, in isolated cell pairs [Neyton & Trautmann, 1985]. Since, for whole cell recording, the cell membrane contributes a large amount of the total current, these records are usually extremely noisy and heavy low pass filtering has to be applied to increase the signal-to-noise ratio to reasonable values. Filtering often reduces the time resolution to levels where conventional kinetic analysis is no more applicable. It is, therefore, necessary to use steady state properties to analyse channel dynamic behaviour. In the cell membrane, gap-junction channels are organized in large clusters of more or less tightly packed channels up to several thousand per plaque [Hülser et al., 1989]. Multichannel recordings for this channel are, therefore, the rule rather than the exception. Current-voltage analysis with this method is well suited for our measurements as reasonable results may be obtained with only a few sweeps of single channel data when multiple channels are present. In addition, it allows discrimination of different channel populations with different gating parameters from their open probability distribution as can be seen in Fig. 8 for gap-junction channels in PLC cells.

Acknowledgement

Beate Rehkopf's expert technical assistance with cell cultures is gratefully acknowledged. We thank Dr. K. Willecke for transfecting HeLa cells, Dr. M.B.A. Djamgoz for carefully reading our manuscript, and R. Rottler for stimulating discussions.

References

Aldrich RW, Yellen G (1983) Analysis of nonstationary channel kinetics. In: Sakmann B, Neher E (eds) Single Channel Recording, Plenum Press, New York, pp 287-299

Beyer EC, Goodenough DA, Paul DL (1988) The connexins, a family of related gap junction proteins. In: Hertzberg EL, Johnson RG (eds) Gap Junctions, Alan R. Liss, Inc., New York, pp 167-175

Beyer EC, Kistler J, Paul DL, Goodenough DA (1989) Antisera directed against connexin43 peptides react with a 43-kD protein localized to gap junctions in myocardium and other tissues. J. Cell Biol. 108: 595-605

Beyer EC, Paul DL, Goodenough DA (1990) Connexin Family of Gap Junction Proteins. J. Membrane Biol. 116: 187-194

Bezanilla F (1985) A high capacity data recording device based on a digital audio processor and a video cassette recorder. Biophys. J. 47: 437-441

Bräuner T, Schmid A, Hülser DF (1990) Tumor Cell Invasion and Gap Junctional Communication I. Normal and Malignant Cells Confronted in Monolayer Cultures. Invasion Metastasis 10: 18-30

Brümmer F, Zempel G, Bühle P, Stein JC, Hülser DF (1991) Retinoic Acid Modulates Gap Junctional Permeability: A Comparative Study of Dye Spreading and Ionic Coupling in Cultured Cells. Exp. Cell Res. 196: 158-163

Caceci MS, Cacheris WP (1984) Fitting curves to data. The simplex algorithm is the answer. BYTE 5: 340-362

Dermietzel R, Traub O, Hwang TK, Beyer E, Bennett MVL, Spray DC, Willecke K (1989) Differential expression of three gap junction proteins in developing and mature brain tissues. Proc. Natl. Acad. Sci. USA 86: 10148-10152

Dunina-Barkovskaya AY, Eckert R, Hülser DF (1992) HeLa - a permanently growing cell line with very low gap junctional coupling. J. Cell Biol. 57, Suppl. 36: 17

Ebihara L, Beyer EC, Swenson KI, Paul DL, Goodenough DA (1989) Cloning and expression of a Xenopus embryonic gap junction protein. Science 243: 1194-1195

Finbow ME, Buultjens TEJ, Serras F, Kam E, John S, Meager L (1988) Immunological and biochemical analysis of the low molecular weight gap junctional proteins. In: Hertzberg EL, Johnson RG (eds) Gap Junctions, Alan R. Liss, Inc., New York, pp 53-67

Gimlich RL, Kumar NM, Gilula NB (1988) Sequence and developmental expression of mRNA coding for a gap junction protein in *Xenopus*. J. Cell Biol. 107: 1065-1073

Gimlich RL, Kumar NM, Gilula NB (1990) Differential Regulation of the Levels of Three Gap Junction mRNAs in *Xenopus* Embryos. J. Cell Biol. 110: 597-605

Haefliger J-A, Bruzzone R, Jenkins NA, Gilbert DJ, Copeland NG, Paul DL (1992) Four Novel Members of the Connexin Family of Gap Junction Proteins. Molecular Cloning, Expression, and Chromosome Mapping. J. Biol. Chem. 267: 2057-2064

Harfst E, Severs NJ, Green CR (1990) Cardiac myocyte gap junctions: evidence for a major connexon protein with an apparent relative molecular mass of 70,000. J. Cell Sci.96: 591-604

Hille B (1984) Ionic Channels of Excitable Membranes. Sinauer Associates. Sunderland Mass.

Hoh JH, John SA, Revel J-P (1991) Molecular Cloning and Characterization of a New Member of the Gap Junction Gene Family, Connexin-31. J. Biol. Chem. 266: 6524-6531

Horn R (1991) Estimating the number of channels in patch recordings. Biophys. J. 60: 433-439

Hülser DF, Paschke D, Greule J (1989) Gap junctions: correlated electrophysiological recordings and ultrastructural analysis by fast freezing and freeze-fracturing. In: Plattner H (ed) Electron Microscopy of Subcellular Dynamics, CRC Press, Inc. Boca Raton, Florida, pp 33-49

Hülser DF, Paschke D, Brümmer F, Eckert R (1990) Characterization of gap junctions by electrophysiological and electronmicroscopical methods. In: Kuczera J, Przestalski S (eds) Biophysics of Membrane Transport, Tenth School Proceedings, Vol. I, Wroclaw, Poland, pp 147-162

Kistler J, Bullivant S (1988) Dissociation of lens fibre gap junctions releases MP70. J. Cell Sci. 91: 415-421

Magleby KL, Stevens CF (1972) The effect of voltage on the time course of end-plate currents. J. Physiol. (London) 223: 151-171

Nelder JA, Mead R (1965) A simplex method for function minimization. Computer J. 7: 308-313

Neyton J, Trautmann A (1985) Single-channel currents of an intercellular junction. Nature 317: 331-335

Moreno AP, Fishman GI, Leinwand LA, Spray DC (1991) Human Connexin43: Changes in Gap Junction Properties After Site-Specific Mutagenesis. Biophys. J. 59: 440a

Paschke D (1989) Gap Junction Kanäle mit unterschiedlichen Leitfähigkeiten. Dissertation, Universität Stuttgart

Paschke D, Eckert R, Hülser DF (1992) High-resolution measurements of gap-junctional conductance during perfusion with anti-connexin antibodies in pairs of cultured mammalian cells. Pflügers Arch. 420: 87-93

Paul DL (1986) Molecular Cloning of cDNA for Rat Liver Gap Junction Protein. J. Cell Biol. 103: 123-134

Press WH, Flannery BP, Teukolsky SA, Vetterling WT (1989) Numerical Recipes in Pascal. The Art of Scientific Computing. Cambridge University Press, Cambridge.

Quade, K (1979) Transformation of Mammalian Cells by Avian Myelocytomatosis Virus and Avian Erythroblastosis Virus. Virology 98: 461-465

Rajewsky MF, Grüneisen A (1972) Cell proliferation in transplanted rat tumors: Influence of the host immune system. Eur. J. Immunol. 2: 445-447

Risek B, Guthrie S, Kumar N, Gilula NB (1990) Modulation of Gap Junction Transcript and Protein Expression during Pregnancy in the Rat. J. Cell Biol. 110: 269-282

Sachs F, Auerbach A (1983) Single channel electrophysiology: Use of the patch clamp. Meth. Enzymol. 103: 147-176

Sansom MSP, Mellor IR (1990) Analysis of the gating of single ion channels using current-voltage surfaces. J. theor. Biol. 144: 213-223

Schwarze W, Kolb H-A (1984) Voltage-dependent kinetics of an ionic channel of large unit conductance in macrophages and myotube membranes. Pflügers Arch. 402: 281-291

Stühmer W (1990) Molecular and patch-clamp approaches to the structure-function relationships of voltage gated channels. Membrane Techn. 64: 1-8

Traub O, Look J, Dermietzel R, Brummer F, Hülser D, Willecke K (1989) Comparative characterization of the 21-kD and 26-kD gap junction proteins in murine liver and cultured hepatocytes. J. Cell. Biol. 108: 1039-1051

Willecke K, Jungbluth S, Dahl E, Hennemann H, Heynkes R, Grzeschik K-H (1990) Six genes of the human connexin gene family coding for gap junctional proteins are assigned to four different human chromosomes. Eur. J. Cell Biol. 53: 275-280

Willecke K, Hennemann H, Dahl E, Jungbluth S, Heynkes R (1991a) The diversity of connexin genes encoding gap junctional proteins. Eur. J. Cell Biol. 56: 1-7

Willecke K, Heynkes R, Dahl E, Stutenkemper R, Hennemann H, Jungbluth S, Suchyna T, Nicholson BJ (1991b) Mouse Connexin37: Cloning and Functional Expression of a Gap Junction Gene Highly Expressed in Lung. J. Cell Biol. 114: 1049-1057

Winterhager E, Stutenkemper R, Traub O, Beyer E, Willecke K (1991) Expression of different connexin genes in rat uterus during decidualization and at term. Eur. J. Cell Biol. 55: 133-142

Yellen G (1982) Single Ca^{2+}-activated nonselective cation channels in neuroblastoma. Nature. 296: 357-359